Bull. Soc. R. Sci. Liège, 2024, **93**(2), 123–133 *Peer-reviewed conference paper*
doi:10.25518/0037-9565.11621

Analytical Lightcurves for Transiting Exomoons

Suman SAHA[1,2]

[1] Indian Institute of Astrophysics, II Block, Koramangala, Bengaluru, India
[2] Instituto de Estudios Astrofísicos, Facultad de Ingeniería y Ciencias, Universidad Diego Portales, Av. Ejército Libertador 441, Santiago, Chile
Correspondence to: suman.saha@mail.udp.cl

Paper presented at the 3rd BINA Workshop on "Scientific Potential of the Indo-Belgian Cooperation", held at the Graphic Era Hill University, Bhimtal (India), 22nd–24th March 2023.

Abstract

Transit photometry has remained the most effective technique to detect and characterize exoplanets. As thousands of exoplanets have been discovered in the last few decades, the possibility of the existence of exomoons in some of these systems can not be avoided. However, the detection of exomoons has still remained elusive, owing to their much smaller expected size compared to their planetary host. With the advent of next generation space telescopes and large ground based telescopes, the possibility to detect them is imminent in near future. In such scenario, a comprehensive analytical formalism to model the transit lightcurves of a transiting exomoon hosting system will be necessary to confirm their detection and study their physical and dynamical characteristics. Here, I present such an analytical formulation, that can be used to simulate the transit lightcurves for an exoplanetary system hosting transiting exomoons. This formalism uses the physical and orbital properties of the three-body star-planet-moon system, to solve their orbital dynamics, and model the transit lightcurves for every possible physical scenarios. In this report, various aspects of this analytical formalism has been discussed, and the model lightcurves for a few of the practical scenarios have been presented.

Keywords: Exoplanets, Exomoons, Transit photometry

1. Introduction

Thousands of exoplanets have been discovered over the past few decades, using various ground-based (e.g., SuperWASP (Pollacco et al., 2006), HATNet (Bakos et al., 2004), KELT (Pepper et al., 2007), etc.) as well as space-based (e.g., CoRoT (Auvergne et al., 2009), Kepler (Borucki et al., 2010) and TESS (Ricker et al., 2015)) facilities. However, majority of these exoplanets have been discovered using the transit method. Transit method have a major advantage over the other exoplanet detection methods, which is the capability to monitor a large number of potential host stars photometrically, leveraging survey telescopes of very large field-of-view. This statistically increases the probability of detecting a large number of undiscovered planetary

bodies using this method. The transit method also allows to study several key physical properties of the detected exoplanets, such as the radius, the orbital inclination and the orbital distance from the host star, as well as the limb-darkening coefficients of the host star. Combining with the spectroscopic observation to study the radial velocity of the host star, the transit method also helps to determine the mass of the exoplanets accurately.

Although the discovery of a large number of exoplanets have been possible through transit and other methods, the discovery of exomoons have still remained elusive. In the recent past, several investigations invoking various techniques have been undertaken to discover exomoons. Apart from the traditional transit method, some of the other techniques that have been proposed over the years for the detection of exomoons are: Transit-Timing Variation (TTV, Sartoretti and Schneider, 1999; Szabó et al., 2006), Transit-Duration Variation (TDV, Kipping, 2009), photometric orbital sampling effect (Heller, 2014; Teachey et al., 2018), imaging of mutual transits (Cabrera and Schneider, 2007), microlensing (Han and Han, 2002), spectroscopy (Williams and Knacke, 2004; Johnson and Huggins, 2006; Oza et al., 2019), polarimetry of self-luminous exoplanets (Sengupta and Marley, 2016), doppler monitoring of directly imaged exoplanets (Agol et al., 2015), pulsar timing (Lewis et al., 2008) and radio emissions of giant exoplanets (Noyola et al., 2014, 2016). Although some of these techniques have resulted in a few exomoon candidates, no confirmed exomoon has yet been recorded.

The major factor behind this non-discovery of exomoons can be attributed to the size of natural satellites, which tends to be much smaller than the planets. However, with the advent of latest state-of-the-art facilities, such as the James Webb Space Telescope (JWST), it might be possible to detect such small exomoons. In order to model such observational data to detect transiting exomoons and characterize their physical properties, a comprehensive analytical formalism would be necessary. The formalism has also to be unambiguous enough to be applicable to all the possible realistic scenarios of dynamical alignments of the star-planet-moon three body system. Here I present such an analytical formalism to simulate and model the transit lightcurves of a planetary system hosting transiting exomoons. The formalism uses the physical and orbital properties of the star-planet-moon three body system to solve their orbital dynamics. I have discussed different aspects of the formalism, that can be applicable to all possible physical alignments of the system, while also keeping it mathematically simple and straightforward, so that it can be applicable to modeling the actual observational data with relative ease.

In Sect. 2, I have discussed theoretical details of the analytical model, and in Sect. 3, I have presented the model lightcurves for a few practical scenarios along with other discussions.

2. Analytical Formalism

It is not possible to analytically solve the dynamics of a three-body system consisting of the star, the planet and the moon directly. So, I consider that the barycenter of the planet-moon system follows a similar orbit as the planet would have followed in the absence of a moon. It must be noted that the barycenter of the planet-moon system always falls within the surface of the planet. For the cases where the moon has mass equal to a significant fraction of the mass

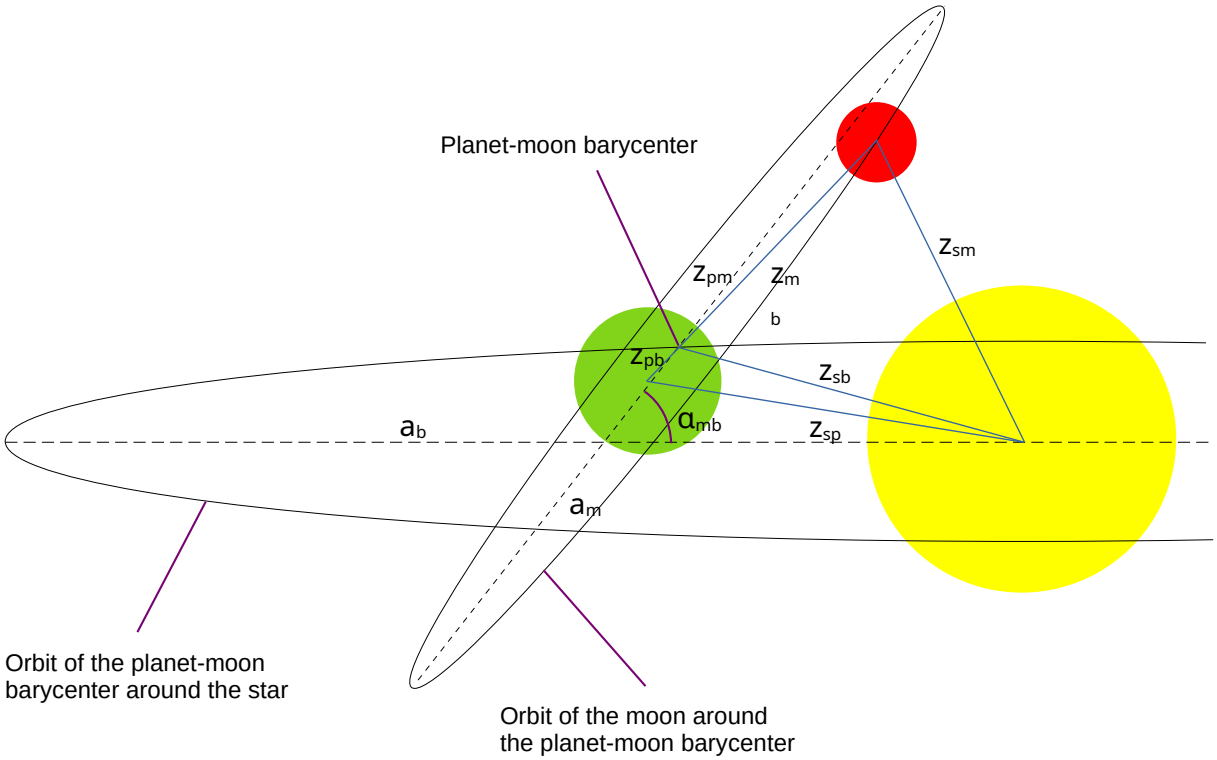

Figure 1: Orbital orientation of the star-planet-moon system from the observer's point of view, showing z_{sp}, z_{pm} and z_{sm}, the separations between the centers of the star and the planet, the planet and the moon, and the star and the moon respectively; z_{sb}, z_{pb} and z_{mb}, the separation of the planet-moon barycenter from the centers of the star, the planet and the moon respectively; α_{mb}, the angle between the major axes of the projected orbits of the planet-moon barycenter around the star and the moon around the planet-moon barycenter; a_b and a_m, the orbital semi-major axes of the planet-moon barycenter around the star and the moon around the planet-moon barycenter respectively.

of the planet, the barycenter would fall at a significant distance from the center of the planet, although being with in the surface of the planet. For the cases where the planet is much more massive than the moon, the barycenter would fall close to the center of the planet. The orbits of the planet and the moon around their common barycenter are assumed to be circular, which is practically the case for most of the moons which are tidally locked.

Now, let's consider a system (cf. Fig. 1) consisting of a planet with radius r_p and a moon with radius r_m, where all the lengths are scaled in terms of the stellar radius. In this case, the separation of the barycenter of the planet-moon system from the center of the star is given by

$$z_{sb} = a_b \sqrt{\sin^2 \theta_b + \cos^2 \theta_b \cos^2 i_b}$$

$$\theta_b = \frac{2\pi}{P_b}(t - t_{0b})$$

where a_b is the semi-major axis, i_b is the inclination angle, θ_b is the orbital phase, P_b is the

orbital period, and t_{0b} is the mid-transit time of the planet-moon barycenter around the star.

The distance of the center of the moon from the planet-moon barycenter is, $a_m = r_{pm}/(1 + M_m/M_p)$, where r_{pm} is the distance between centers of the moon and the planet, M_m is the mass of the moon and M_p is the mass of the planet. The distance of the center of the planet from the planet-moon barycenter can be written as, $a_p = r_{pm} - a_m$.

Now, the separation between the center of the moon and the barycenter of the planet-moon system is given by

$$z_{mb} = a_m \sqrt{\sin^2 \theta_m + \cos^2 \theta_m \cos^2 i_m}$$

$$\theta_m = \frac{2\pi}{P_m}(t - t_{0m})$$

and the separation of the center of the planet from the barycenter of the planet-moon system is given by

$$z_{pb} = a_p \sqrt{\sin^2 \theta_m + \cos^2 \theta_m \cos^2 i_m},$$

where i_m is the orbital inclination angle, θ_m is the orbital phase, P_m is the orbital period, and t_{0m} is the mid-transit time of the moon around the planet-moon barycenter. The separation between the center of the planet and the center of the moon can be written as

$$z_{pm} = z_{mb} + z_{pb}.$$

In order to combine these definitions from the planet-moon two-body system with the system consisting of the star and the planet-moon barycenter, I denote the angle between the major axes of the projected orbits of the planet-moon barycenter around the star and the moon around the planet-moon barycenter as α_{mb}. In this case, the separation between the centers of the planet and the star can be written as

$$z_{sp} = \sqrt{z_{sb}^2 + z_{pb}^2 - 2 z_{sb} z_{pb} \cos \phi}$$

$$\phi = \alpha_{mb} + \eta - \eta_1$$

$$\eta = \begin{cases} \cos^{-1}\left(\dfrac{\cos\theta_b \cos i_b}{\sqrt{\sin^2\theta_b + \cos^2\theta_b \cos^2 i_b}}\right), & 0 \le \theta_b \le \pi \\ -\cos^{-1}\left(\dfrac{\cos\theta_b \cos i_b}{\sqrt{\sin^2\theta_b + \cos^2\theta_b \cos^2 i_b}}\right), & -\pi \le \theta_b < 0 \end{cases}$$

$$\eta_1 = \begin{cases} \cos^{-1}\left(\dfrac{\cos\theta_m \cos i_m}{\sqrt{\sin^2\theta_m + \cos^2\theta_m \cos^2 i_m}}\right), & 0 \le \theta_m \le \pi \\ -\cos^{-1}\left(\dfrac{\cos\theta_m \cos i_m}{\sqrt{\sin^2\theta_m + \cos^2\theta_m \cos^2 i_m}}\right), & -\pi \le \theta_m < 0 \end{cases}$$

where ϕ is the angle between z_{sb} and z_{pb}. Similarly, the separation between the centers of the moon and the star is written as

$$z_{sm} = \sqrt{z_{sb}^2 + z_{mb}^2 - 2z_{sb}z_{mb}\cos\phi_1}$$

$$\phi_1 = \pi - \phi$$

If the ratio between the mass of the moon and the planet is assumed very small, the barycenter of the planet-moon system could be approximated at the center of the planet, i.e. $a_p = 0$, in which case the model simplifies to $z_{pb} = 0$, $z_{sp} = z_{sb}$ and $z_{pm} = z_{mb}$.

Apart from these separations between the centers of the three circular bodies, the separation of the center of each body from the points of intersection of the two other bodies would be required to solve the conditions for all possible dynamical alignments. The separation of the star from the points of intersection of the moon and the planet are given by

$$l_{1s} = \sqrt{r_p^2 + z_{sp}^2 - 2r_p z_{sp}\cos\left(\cos^{-1}\left(\frac{z_{sp}^2 + z_{pm}^2 - z_{sm}^2}{2z_{sp}z_{pm}}\right) + \cos^{-1}\left(\frac{r_p^2 - r_m^2 + z_{pm}^2}{2z_{pm}r_p}\right)\right)}$$

$$l_{2s} = \sqrt{r_p^2 + z_{sp}^2 - 2r_p z_{sp}\cos\left(\cos^{-1}\left(\frac{z_{sp}^2 + z_{pm}^2 - z_{sm}^2}{2z_{sp}z_{pm}}\right) - \cos^{-1}\left(\frac{r_p^2 - r_m^2 + z_{pm}^2}{2z_{pm}r_p}\right)\right)}$$

Similarly, the separation of the planet from the points of intersection of the moon and the star are given by

$$l_{1p} = \sqrt{r_m^2 + z_{pm}^2 - 2r_m z_{pm}\cos\left(\cos^{-1}\left(\frac{z_{pm}^2 + z_{sm}^2 - z_{sp}^2}{2z_{pm}z_{sm}}\right) + \cos^{-1}\left(\frac{r_m^2 - 1 + z_{sm}^2}{2z_{sm}r_m}\right)\right)}$$

$$l_{2p} = \sqrt{r_m^2 + z_{pm}^2 - 2r_m z_{pm}\cos\left(\cos^{-1}\left(\frac{z_{pm}^2 + z_{sm}^2 - z_{sp}^2}{2z_{pm}z_{sm}}\right) - \cos^{-1}\left(\frac{r_m^2 - 1 + z_{sm}^2}{2z_{sm}r_m}\right)\right)}$$

and, the separation of the moon from the points of intersection of the star and the planet are given by

$$l_{1m} = \sqrt{r_p^2 + z_{pm}^2 - 2r_p z_{pm}\cos\left(\cos^{-1}\left(\frac{z_{pm}^2 + z_{sp}^2 - z_{sm}^2}{2z_{pm}z_{sp}}\right) + \cos^{-1}\left(\frac{r_p^2 - 1 + z_{sp}^2}{2z_{sp}r_p}\right)\right)}$$

$$l_{2m} = \sqrt{r_p^2 + z_{pm}^2 - 2r_p z_{pm}\cos\left(\cos^{-1}\left(\frac{z_{pm}^2 + z_{sp}^2 - z_{sm}^2}{2z_{pm}z_{sp}}\right) - \cos^{-1}\left(\frac{r_p^2 - 1 + z_{sp}^2}{2z_{sp}r_p}\right)\right)}$$

Using these parameters, all the possible alignments of the star-planet-moon system can be categorized into 22 cases (see Saha and Sengupta, 2022, Fig. 3 and Table 1). To account for the limb-darkening effect of the host-star, the analytical quadratic limb-darkening formulation (Mandel and Agol, 2002) can be used for the occultation by the planet, and small-planet approximation can be used for the occultation by the moon.

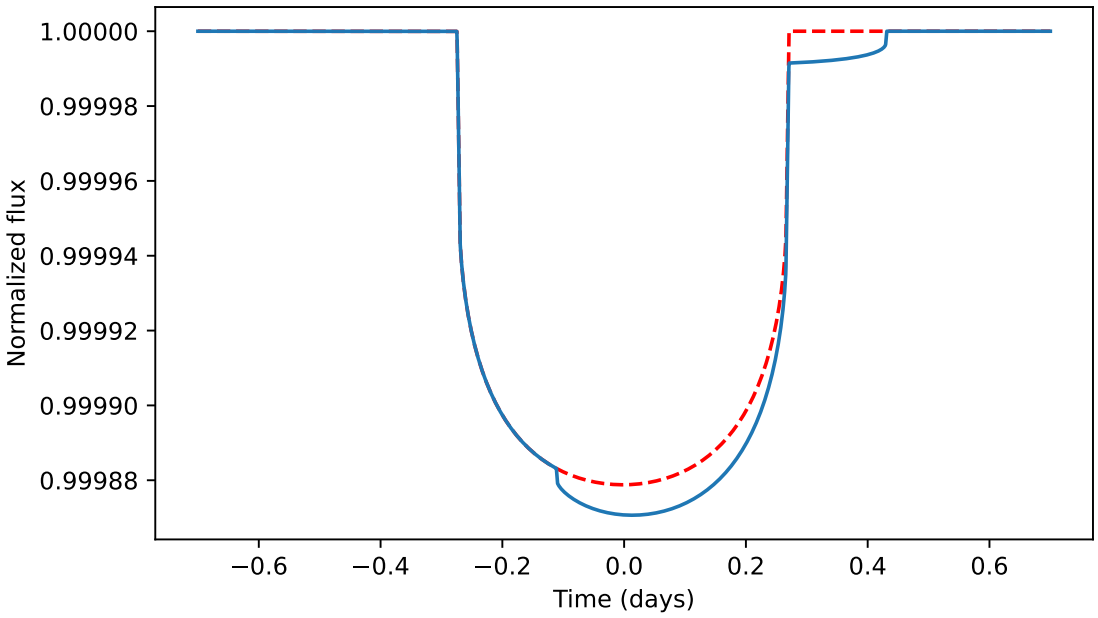

Figure 2: Transit light-curve for a moon hosting exoplanetary system similar to our Sun-Earth-Moon system, with $r_p = 0.01$, $r_m = 0.0027$, $t_{0b} = 0$ days, $t_{0m} = 7$ days, $P_b = 365$ days, $P_m = 27$ days, $a_b = 215$, $r_{pm} = 0.6$, $M_p/M_m = 81$, $i_b = 90^\circ$, $i_m = 90^\circ$, $\alpha_{mb} = 0^\circ$, $u_1 = 0.4$ and $u_2 = 0.25$. The dashed red line shows the transit signature of the planet in the absence of a moon.

3. Results and Discussions

The analytical transit model for a moon hosting planetary system, as described in the last section, consists of parameters r_p, r_m, t_{0b}, t_{0m}, P_b, P_m, a_b, r_{pm}, M_p/M_m, i_b, i_m, α_{mb}, and the limb-darkening coefficients of the host-star. Here, we have considered the quadratic limb darkening coefficients, u_1 and u_2 (Mandel and Agol, 2002).

Now, let's consider a scenario very similar to our Sun-Earth-Moon system. The parameters for this case can be approximated as: $r_p = 0.01$, $r_m = 0.0027$, $t_{0b} = 0$ days, $t_{0m} = 7$ days, $P_b = 365$ days, $P_m = 27$ days, $a_b = 215$, $r_{pm} = 0.6$, $M_p/M_m = 81$, $i_b = 90^\circ$, $i_m = 90^\circ$, $\alpha_{mb} = 0^\circ$, $u_1 = 0.4$ and $u_2 = 0.25$. The transit lightcurve for this scenario is shown in Fig. 2. Here, $i_b = i_m = 90^\circ$ implies that both the planet and the moon are transiting through the center of the star, and that combined with $\alpha_{mb} = 0^\circ$ implies that the orbit of the moon is aligned with the orbit of the planet, i.e., both the planet and the moon are in the same orbital plane. From the figure, the transit signature of the moon can be clearly seen, which lags the transit of the planet for this particular case. In general, the transit of the moon can take place before, during or after the transit of the planet, depending upon a combination of various parameters.

The probability of finding an moon is much high around a giant planet compared to a terrestrial one. Also, massive planets are more likely to host larger moons. Let's consider a

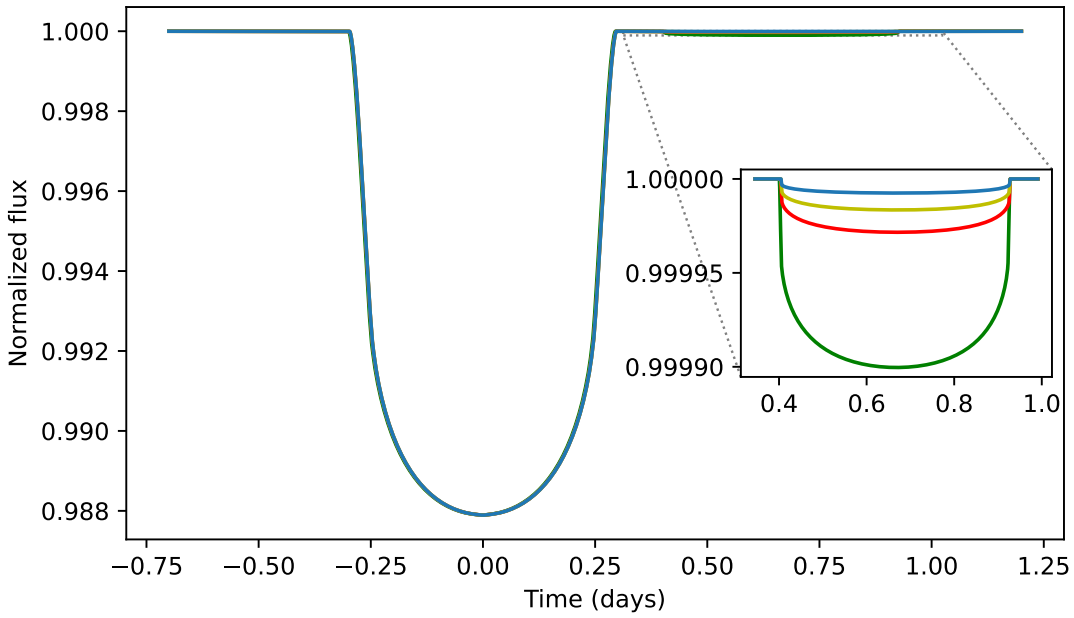

Figure 3: Transit light-curves for transiting system with a Jupiter-like planet around a Sun-like star, hosting moons similar to the Earth (green), Mars (red), Titan (yellow) and Luna (blue). The model parameters are given by: $r_p = 0.01$, $r_{mE} = 0.0091$, $r_{mM} = 0.00484$, $r_{mT} = 0.00369$, $r_{mL} = 0.00249$, $t_{0b} = 0$ days, $t_{0m} = 4$ days, $P_b = 365$ days, $P_m = 14.47$ days, $a_b = 215$, $r_{pm} = 2.5$, $M_p/M_{mE} = 316.7$, $M_p/M_{mM} = 2968.75$, $M_p/M_{mT} = 13571.4$, $M_p/M_{mL} = 25675.7$, $i_b = 90°$, $i_m = 90°$, $\alpha_{mb} = 0°$, $u_1 = 0.4$ and $u_2 = 0.25$.

scenario with a Jupiter-like planet around a Sun-like star orbiting at a distance of 1 AU, i.e. in the habitable zone of the star. Now, let's also consider four different cases of moons, i.e. with sizes similar to Earth, Mars, Titan and Luna (Earth's moon), orbiting around the giant planet. The model parameters for these scenarios can be written as: $r_p = 0.01$, $r_{mE} = 0.0091$, $r_{mM} = 0.00484$, $r_{mT} = 0.00369$, $r_{mL} = 0.00249$, $t_{0b} = 0$ days, $t_{0m} = 4$ days, $P_b = 365$ days, $P_m = 14.47$ days, $a_b = 215$, $r_{pm} = 2.5$, $M_p/M_{mE} = 316.7$, $M_p/M_{mM} = 2968.75$, $M_p/M_{mT} = 13571.4$, $M_p/M_{mL} = 25675.7$, $i_b = 90°$, $i_m = 90°$, $\alpha_{mb} = 0°$, $u_1 = 0.4$ and $u_2 = 0.25$. Here, $i_b = i_m = 90°$. The transit lightcurves for these scenarios are shown in Fig. 3.

Since, the detection of exomoons directly depends on the size of the moon relative to the star, detection of sub-Earth sized exomoons would require extremely precise photometric observations. Such extremely high precision could be be achieved using the next generation large telescopes, such as the James Webb Space Telescope (JWST), the European Extremely Large Telescope (E-ELT), the Thirty Meter Telescope (TMT), and the Giant Magellan Telescope (GMT) etc. Apart from the photometric noise, the correlated noise due to stellar variability and pulsations, and instrumental factors can also pose a challenge in the detection of exomoons. Such noises can be treated using sophisticated techniques like the Gaussian process regression

(Rasmussen and Williams, 2006; Johnson et al., 2015; Saha et al., 2021; Saha and Sengupta, 2021; Saha, 2022, 2023) to minimize their impact on the lightcurves.

Further Information

Author's ORCID identifier

0000-0001-8018-0264 (Suman SAHA)

Conflicts of interest

The author declares no conflict of interest.

References

Agol, E., Jansen, T., Lacy, B., Robinson, T. D. and Meadows, V. (2015) The Center of Light: Spectroastrometric Detection of Exomoons. ApJ, 812(1), 5. https://doi.org/10.1088/0004-637X/812/1/5.

Auvergne, M., Bodin, P., Boisnard, L., Buey, J. T., Chaintreuil, S., Epstein, G., Jouret, M., Lam-Trong, T., Levacher, P., Magnan, A., Perez, R., Plasson, P., Plesseria, J., Peter, G., Steller, M., Tiphène, D., Baglin, A., Agogué, P., Appourchaux, T., Barbet, D., Beaufort, T., Bellenger, R., Berlin, R., Bernardi, P., Blouin, D., Boumier, P., Bonneau, F., Briet, R., Butler, B., Cautain, R., Chiavassa, F., Costes, V., Cuvilho, J., Cunha-Parro, V., de Oliveira Fialho, F., Decaudin, M., Defise, J. M., Djalal, S., Docclo, A., Drummond, R., Dupuis, O., Exil, G., Fauré, C., Gaboriaud, A., Gamet, P., Gavalda, P., Grolleau, E., Gueguen, L., Guivarc'h, V., Guterman, P., Hasiba, J., Huntzinger, G., Hustaix, H., Imbert, C., Jeanville, G., Johlander, B., Jorda, L., Journoud, P., Karioty, F., Kerjean, L., Lafond, L., Lapeyrere, V., Landiech, P., Larqué, T., Laudet, P., Le Merrer, J., Leporati, L., Leruyet, B., Levieuge, B., Llebaria, A., Martin, L., Mazy, E., Mesnager, J. M., Michel, J. P., Moalic, J. P., Monjoin, W., Naudet, D., Neukirchner, S., Nguyen-Kim, K., Ollivier, M., Orcesi, J. L., Ottacher, H., Oulali, A., Parisot, J., Perruchot, S., Piacentino, A., Pinheiro da Silva, L., Platzer, J., Pontet, B., Pradines, A., Quentin, C., Rohbeck, U., Rolland, G., Rollenhagen, F., Romagnan, R., Russ, N., Samadi, R., Schmidt, R., Schwartz, N., Sebbag, I., Smit, H., Sunter, W., Tello, M., Toulouse, P., Ulmer, B., Vandermarcq, O., Vergnault, E., Wallner, R., Waultier, G. and Zanatta, P. (2009) The CoRoT satellite in flight: description and performance. A&A, 506(1), 411–424. https://doi.org/10.1051/0004-6361/200810860.

Bakos, G., Noyes, R. W., Kovács, G., Stanek, K. Z., Sasselov, D. D. and Domsa, I. (2004) Wide-Field Millimagnitude Photometry with the HAT: A Tool for Extrasolar Planet Detection. PASP, 116(817), 266–277. https://doi.org/10.1086/382735.

Borucki, W. J., Koch, D., Basri, G., Batalha, N., Brown, T., Caldwell, D., Caldwell, J., Christensen-Dalsgaard, J., Cochran, W. D., DeVore, E., Dunham, E. W., Dupree, A. K., Gautier, T. N., Geary, J. C., Gilliland, R., Gould, A., Howell, S. B., Jenkins, J. M., Kondo, Y., Latham, D. W., Marcy, G. W., Meibom, S., Kjeldsen, H., Lissauer, J. J., Monet, D. G., Morrison, D., Sasselov, D., Tarter, J., Boss, A., Brownlee, D., Owen, T., Buzasi, D., Charbonneau, D., Doyle, L., Fortney, J., Ford, E. B., Holman, M. J., Seager, S., Steffen, J. H., Welsh, W. F., Rowe, J., Anderson, H., Buchhave, L., Ciardi, D., Walkowicz, L., Sherry, W., Horch, E., Isaacson, H., Everett, M. E., Fischer, D., Torres, G., Johnson, J. A., Endl, M., MacQueen, P., Bryson, S. T., Dotson, J., Haas, M., Kolodziejczak, J., Van Cleve, J., Chandrasekaran, H., Twicken, J. D., Quintana, E. V., Clarke, B. D., Allen, C., Li, J., Wu, H., Tenenbaum, P., Verner, E., Bruhweiler, F., Barnes, J. and Prsa, A. (2010) Kepler Planet-Detection Mission: Introduction and First Results. Sci, 327(5968), 977. https://doi.org/10.1126/science.1185402.

Cabrera, J. and Schneider, J. (2007) Detecting companions to extrasolar planets using mutual events. A&A, 464(3), 1133–1138. https://doi.org/10.1051/0004-6361:20066111.

Han, C. and Han, W. (2002) On the Feasibility of Detecting Satellites of Extrasolar Planets via Microlensing. ApJ, 580(1), 490–493. https://doi.org/10.1086/343082.

Heller, R. (2014) Detecting Extrasolar Moons Akin to Solar System Satellites with an Orbital Sampling Effect. ApJ, 787(1), 14. https://doi.org/10.1088/0004-637X/787/1/14.

Johnson, M. C., Cochran, W. D., Collier Cameron, A. and Bayliss, D. (2015) Measurement of the Nodal Precession of WASP-33 b via Doppler Tomography. ApJ, 810(2), L23. https://doi.org/10.1088/2041-8205/810/2/L23.

Johnson, R. E. and Huggins, P. J. (2006) Toroidal Atmospheres around Extrasolar Planets. PASP, 118(846), 1136–1143. https://doi.org/10.1086/506183.

Kipping, D. M. (2009) Transit timing effects due to an exomoon. MNRAS, 392(1), 181–189. https://doi.org/10.1111/j.1365-2966.2008.13999.x.

Lewis, K. M., Sackett, P. D. and Mardling, R. A. (2008) Possibility of Detecting Moons of Pulsar Planets through Time-of-Arrival Analysis. ApJ, 685(2), L153. https://doi.org/10.1086/592743.

Mandel, K. and Agol, E. (2002) Analytic Light Curves for Planetary Transit Searches. ApJ, 580(2), L171–L175. https://doi.org/10.1086/345520.

Noyola, J. P., Satyal, S. and Musielak, Z. E. (2014) Detection of Exomoons through Observation of Radio Emissions. ApJ, 791(1), 25. https://doi.org/10.1088/0004-637X/791/1/25.

Noyola, J. P., Satyal, S. and Musielak, Z. E. (2016) On the Radio Detection of Multiple-exomoon Systems due to Plasma Torus Sharing. ApJ, 821(2), 97. https://doi.org/10.3847/0004-637X/821/2/97.

Oza, A. V., Johnson, R. E., Lellouch, E., Schmidt, C., Schneider, N., Huang, C., Gamborino, D., Gebek, A., Wyttenbach, A., Demory, B.-O., Mordasini, C., Saxena, P., Dubois, D., Moullet, A. and Thomas, N. (2019) Sodium and Potassium Signatures of Volcanic Satellites Orbiting Close-in Gas Giant Exoplanets. ApJ, 885(2), 168. https://doi.org/10.3847/1538-4357/ab40cc.

Pepper, J., Pogge, R. W., DePoy, D. L., Marshall, J. L., Stanek, K. Z., Stutz, A. M., Poindexter, S., Siverd, R., O'Brien, T. P., Trueblood, M. and Trueblood, P. (2007) The Kilodegree Extremely Little Telescope (KELT): A Small Robotic Telescope for Large-Area Synoptic Surveys. PASP, 119(858), 923–935. https://doi.org/10.1086/521836.

Pollacco, D. L., Skillen, I., Collier Cameron, A., Christian, D. J., Hellier, C., Irwin, J., Lister, T. A., Street, R. A., West, R. G., Anderson, D. R., Clarkson, W. I., Deeg, H., Enoch, B., Evans, A., Fitzsimmons, A., Haswell, C. A., Hodgkin, S., Horne, K., Kane, S. R., Keenan, F. P., Maxted, P. F. L., Norton, A. J., Osborne, J., Parley, N. R., Ryans, R. S. I., Smalley, B., Wheatley, P. J. and Wilson, D. M. (2006) The WASP Project and the SuperWASP Cameras. PASP, 118(848), 1407–1418. https://doi.org/10.1086/508556.

Rasmussen, C. E. and Williams, C. K. I. (2006) Gaussian Processes for Machine Learning. The MIT Press.

Ricker, G. R., Winn, J. N., Vanderspek, R., Latham, D. W., Bakos, G. Á., Bean, J. L., Berta-Thompson, Z. K., Brown, T. M., Buchhave, L., Butler, N. R., Butler, R. P., Chaplin, W. J., Charbonneau, D., Christensen-Dalsgaard, J., Clampin, M., Deming, D., Doty, J., De Lee, N., Dressing, C., Dunham, E. W., Endl, M., Fressin, F., Ge, J., Henning, T., Holman, M. J., Howard, A. W., Ida, S., Jenkins, J. M., Jernigan, G., Johnson, J. A., Kaltenegger, L., Kawai, N., Kjeldsen, H., Laughlin, G., Levine, A. M., Lin, D., Lissauer, J. J., MacQueen, P., Marcy, G., McCullough, P. R., Morton, T. D., Narita, N., Paegert, M., Palle, E., Pepe, F., Pepper, J., Quirrenbach, A., Rinehart, S. A., Sasselov, D., Sato, B., Seager, S., Sozzetti, A., Stassun, K. G., Sullivan, P., Szentgyorgyi, A., Torres, G., Udry, S. and Villasenor, J. (2015) Transiting Exoplanet Survey Satellite (TESS). JATIS, 1, 014003. https://doi.org/10.1117/1.JATIS.1.1.014003.

Saha, S. (2022) Precise Transit Photometric Studies of Exoplanets and Exomoons. Ph.D. thesis, Indian Institute of Astrophysics.

Saha, S. (2023) Precise Transit Photometry Using TESS: Updated Physical Properties for 28 Exoplanets around Bright Stars. ApJS, 268(1), 2. https://doi.org/10.3847/1538-4365/acdb6b.

Saha, S., Chakrabarty, A. and Sengupta, S. (2021) Multiband Transit Follow-up Observations of Five Hot Jupiters with Critical Noise Treatments: Improved Physical Properties. AJ, 162(1), 18. https://doi.org/10.3847/1538-3881/ac01dd.

Saha, S. and Sengupta, S. (2021) Critical Analysis of Tess Transit Photometric Data: Improved Physical Properties for Five Exoplanets. AJ, 162(5), 221. https://doi.org/10.3847/1538-3881/ac294d.

Saha, S. and Sengupta, S. (2022) Transit Light Curves for Exomoons: Analytical Formalism. ApJ, 936(1), 2. https://doi.org/10.3847/1538-4357/ac85a9.

Sartoretti, P. and Schneider, J. (1999) On the detection of satellites of extrasolar planets with the method of transits. A&AS, 134, 553–560. https://doi.org/10.1051/aas:1999148.

Sengupta, S. and Marley, M. S. (2016) Detecting Exomoons around Self-luminous Giant Exoplanets through Polarization. ApJ, 824(2), 76. https://doi.org/10.3847/0004-637X/824/2/76.

Szabó, G. M., Szatmáry, K., Divéki, Z. and Simon, A. (2006) Possibility of a photometric detection of "exomoons". A&A, 450(1), 395–398. https://doi.org/10.1051/0004-6361:20054555.

Teachey, A., Kipping, D. M. and Schmitt, A. R. (2018) HEK. VI. On the Dearth of Galilean Analogs in Kepler, and the Exomoon Candidate Kepler-1625b I. AJ, 155(1), 36. https://doi.org/10.3847/1538-3881/aa93f2.

Williams, D. M. and Knacke, R. F. (2004) Looking for Planetary Moons in the Spectra of Distant Jupiters. AsBio, 4(3), 400–403. https://doi.org/10.1089/ast.2004.4.400.